doi：10. 12068/j. issn. 1005－3026. 2026. 20269027

时滞攻击下复值多智能体系统的输出包围控制

刘 坚，聂鸿基
（济南大学 数学科学学院，山东 济南 250022）

摘 要：针对网络攻击破坏系统安全稳定运行的问题，本文从防御者角度进行了时滞攻击下复值非线性多智能体系统的输出包围一致性安全控制研究．首先，针对跟随者状态难以直接获取的问题，设计分布式状态观测器以实现精准估计．其次，时滞攻击通过恶意延迟数据包传输，其累积效应会破坏系统协同稳定性，甚至诱发失稳；多领导者凸包的时变特性与时滞–非线性强耦合相结合，进一步加剧了稳定性分析难度．为此，区别于传统观测器同步控制，本文设计分布式切换控制协议，将受攻击误差系统建模为切换系统．进一步，运用复域Lyapunov函数方法与不等式技巧，推导出误差系统渐近收敛的充分条件，确保系统在时滞攻击下实现输出包围一致性．最后，利用数值算例验证了所提方法的有效性．

关 键 词：时滞攻击；观测器；系统误差；多智能体系统；包围控制
中图分类号：TP 13 **文献标志码**：A **文章编号**：1005-3026(2026)07-0040-08

Output Containment Control of Complex-Valued Multi-agent Systems Under Time-Delay Attacks

LIU Jian, *NIE Hong-ji*
(School of Mathematical Sciences, University of Jinan, Jinan 250022, China. Corresponding author: LIU Jian, E-mail: ss_liuj@ujn.edu.cn)

Abstract: To address the issue of network attacks disrupting the safe and stable operation of systems, the secure output containment consensus control of complex-valued nonlinear multi-agent systems under time-delay attacks was investigated from the defender's perspective. Firstly, since the states of the followers are difficult to obtain directly, a distributed state observer was designed to achieve precise estimation. Secondly, data packet transmission was maliciously delayed by time-delay attacks, whose cumulative effect damaged the cooperative stability of the system and even caused instability. The time-varying property of the convex hull composed of multiple leaders and the strong coupling between time delay and nonlinearity further raised the difficulty of stability analysis. Distinguished from traditional observer-based synchronization control, a distributed switching control protocol was designed, and the attacked error system was modeled as a switching system. With the adoption of complex-domain Lyapunov function method and inequality techniques, sufficient conditions for the asymptotic convergence of the error system were derived to ensure the realization of output containment consensus against time-delay attacks, and numerical examples were finally provided to verify the effectiveness of the proposed method.

Key words: time-delay attack; observer; system error; multi-agent system; containment control

多智能体系统(multi-agent systems, MASs)的分布式协同控制在无人机编队、工业集群调度等领域应用广泛．其中，包围控制作为一种协同策略，针对由多个领导者和多个跟随者构成的多智能体系统，设计合适的控制协议使跟随者进入由领导者张成的凸包内，在无人机协同避障、灾

收稿日期：2026-03-25
基金项目：山东省自然科学基金资助项目(ZR2024MF105)．
作者简介：刘 坚(1970—)，女，山东滨州人，济南大学教授．
通信作者：刘 坚，E-mail：ss_liuj@ujn.edu.cn.

害救援中的安全区域控制等实际工程中发挥着重要作用,因而受到广泛关注[1−2].2006年,Ferrari-Trecate等[1]首次提出“停−走”控制策略实现跟随者渐近进入凸包;随后Xiao等[2]针对异构系统提出间歇控制算法.

值得注意的是,多数控制技术依赖系统状态信息,然而在实际中,受测量精度和信道约束的影响,真实状态往往难以直接获取.状态观测器融合输出信息实现状态估计,为该问题提供了有效解决方案[3−4].文献[3]针对领导者输入未知的情况,设计了分布式自适应观测器实现有向拓扑下非线性系统的输出包围控制;文献[4]针对跟随者状态未知的情况,设计了观测器实现时滞复值系统的包围控制.

多智能体系统的协同控制依赖于信息交互,通信安全至关重要.随着网络通信技术与多智能体系统的深度融合,系统不再处于封闭状态,信息传输过程中可能面临入侵、篡改、伪造等恶意攻击,以及数据包延迟等一系列问题,从而严重威胁系统的安全性与协同性能.目前,针对网络攻击下多智能体系统的安全一致性控制已取得一些成果[5−10].文献[5]研究链路攻击下复值系统的安全一致性;文献[6]利用事件触发机制实现拒绝服务攻击下的包围控制;文献[7−8]考虑欺骗攻击,其中文献[7]设计自适应观测器实现异构系统的输出包围控制;文献[9−10]考虑时滞攻击,其中文献[9]针对电力系统设计了鲁棒控制策略以缓解时滞攻击的影响.

然而,现有研究主要关注链路攻击、拒绝服务攻击或欺骗攻击,尚未考虑时滞攻击下的输出包围一致性问题,尤其是复值非线性多智能体系统.链路攻击和拒绝服务攻击通过破坏链路或耗尽资源阻断通信;欺骗攻击通过篡改数据误导决策;而时滞攻击是一种隐蔽的内部攻击,通过恶意延迟数据包传输,不显式修改数据或阻断链路,因而易于实施且难以检测,其累积效应可能破坏系统稳定性甚至诱发失稳.值得注意的是,现有时滞攻击研究[9−10]仅针对单领导者,未涉及多领导者场景下的包围控制.领导者带来的凸包动态变化、跟随者对多个领导者轨迹的同步需求,以及时滞攻击下信息交互的非同步性,均使得问题更加复杂.

另一方面,复值多智能体系统的研究具有与实值系统同等重要的理论价值与应用前景.复值能同时表征幅值与相位信息,在量子控制、电磁分析等领域具有优势;此外,复值神经网络展现出更出色的网络学习能力和自组织能力,在图像处理、信号预测等任务中表现优异.文献[11]实现了时滞复值多智能体系统的领导者−跟随者同步;文献[4]研究了链路攻击和拒绝服务攻击下的复值多智能体系统包围控制.然而,时滞攻击下的复值多智能体系统包围控制问题尚未解决.时滞攻击的隐蔽性、多领导者凸包的时变性,以及时滞与复数域非线性动力学的强耦合,大大增加了稳定性分析的复杂性.具体而言,复值系统需同时处理实部与虚部的耦合,时滞攻击引入的不确定延迟进一步破坏了同步条件,使传统Lyapunov−Krasovskii方法或线性矩阵不等式(LMI)框架面临新挑战.

针对时滞攻击下复值多智能体系统的安全包围一致性控制这一亟待解决的难题,本文设计了分布式状态观测器与弹性控制协议.其主要贡献如下:1)研究复值非线性多智能体系统的包围一致性问题,拓展该类系统在实际场景中的应用范围,并设计复数域分布式状态观测器实现对跟随者状态的精确估计;2)首次解决时滞攻击下多智能体系统的包围一致性问题,依据时滞攻击特性设计分布式切换控制协议,将受攻击系统建模为复值切换系统;3)运用复域Lyapunov理论与不等式技巧,推导包围控制的充分判据,确保跟随者输出收敛至多个领导者所张成的凸包内,从而实现时滞攻击下的精确包围控制.

符号说明:$\boldsymbol{C}^n$和$\boldsymbol{C}^{p\times q}$分别表示$n$维复列向量和$p\times q$阶复矩阵;$\|\cdot\|$代表欧几里得范数;符号$\otimes$表示Kronecker积;对于矩阵$\boldsymbol{A}$(或者向量$\boldsymbol{x}$),$\boldsymbol{A}^{\mathrm{T}}$(或者$\boldsymbol{x}^{\mathrm{T}}$)表示矩阵$\boldsymbol{A}$的转置矩阵(或者向量$\boldsymbol{x}$的转置向量),$\boldsymbol{A}^{\mathrm{H}}$(或者$\boldsymbol{x}^{\mathrm{H}}$)表示矩阵$\boldsymbol{A}$的共轭转置矩阵(或者向量$\boldsymbol{x}$的共轭转置向量),同时$\boldsymbol{A}^{\mathrm{S}}=\boldsymbol{A}^{\mathrm{H}}+\boldsymbol{A}$;$\boldsymbol{0}_{p\times q}$表示所有元素都是0的$p\times q$阶矩阵,$\boldsymbol{I}_N$代表$N$阶单位矩阵;定义$\lambda_{\min}(\boldsymbol{A})$和$\lambda_{\max}(\boldsymbol{A})$分别为矩阵$\boldsymbol{A}$的最小特征值和最大特征值;对于任意复数$y$,利用$y^{\mathrm{r}}$和$y^{\mathrm{i}}$分别表示该复数的实部和虚部,即$y=y^{\mathrm{r}}+\mathrm{j}y^{\mathrm{i}}$,其中$\mathrm{j}=\sqrt{-1}$为虚数单位;$\mathrm{dist}(\boldsymbol{x},\boldsymbol{\Omega})$表示从$\boldsymbol{x}\in\boldsymbol{C}^n$到集合$\boldsymbol{\Omega}\subseteq\boldsymbol{C}^n$在欧几里得范数下的距离,即$\mathrm{dist}(\boldsymbol{x},\boldsymbol{\Omega})=\inf\limits_{\boldsymbol{y}\in\boldsymbol{\Omega}}\|\boldsymbol{x}-\boldsymbol{y}\|_2$.

代数图论:令图$G=(V,E,\boldsymbol{A})$代表多智能体系统的拓扑结构,其中多智能体系统中包含N个跟随者以及M个领导者.图像节点集$V=\{1,\cdots,N+M\}$,边集$E\subseteq V\times V$;同时,加权邻接矩阵$\boldsymbol{A}=$

$\left[a_{ij}\right]_{(N+M)\times(N+M)}$ 满足：若$(j,i)\in E$，则$a_{ij}>0$，否则$a_{ij}=0$. 度矩阵表示为$\boldsymbol{D}=\mathrm{diag}\{d_1,\cdots,d_{N+M}\}$，其中$d_i=\sum_{j=1}^{N}a_{ij}$；Laplacian 矩阵$\boldsymbol{L}=\left[l_{ij}\right]_{(N+M)\times(N+M)}$，定义$\boldsymbol{L}=\boldsymbol{D}-\boldsymbol{A}$. 由于领导者不接收来自跟随者的输出，所以$\boldsymbol{L}=\begin{bmatrix}\boldsymbol{L}_1 & \boldsymbol{L}_2\\ \boldsymbol{0}_{M\times N} & \boldsymbol{0}_{M\times N}\end{bmatrix}$.

1 问题阐述与预备知识

1.1 系统模型

考虑具有N个跟随者和M个领导者的非线性多智能体系统. 其中，第i个跟随者方程为

$$\left.\begin{aligned}\dot{\boldsymbol{x}}_i(t)&=\boldsymbol{A}\boldsymbol{x}_i(t)+\boldsymbol{B}\boldsymbol{u}_i(t)+\boldsymbol{f}(t,\boldsymbol{x}_i(t)),\\ \boldsymbol{y}_i(t)&=\boldsymbol{C}\boldsymbol{x}_i(t).\end{aligned}\right\}\tag{1}$$

其中：$i\in\{1,2,\cdots,N\}$；t表示时间；$\boldsymbol{x}_i(t)\in\boldsymbol{C}^n$，$\boldsymbol{u}_i(t)\in\boldsymbol{C}^p$，$\boldsymbol{y}_i(t)\in\boldsymbol{C}^m$分别表示第$i$个跟随者的状态向量、控制输入和测量输出. 同时，矩阵$\boldsymbol{A}\in\boldsymbol{C}^{n\times n}$，$\boldsymbol{B}\in\boldsymbol{C}^{n\times p}$，$\boldsymbol{C}\in\boldsymbol{C}^{m\times n}$，$\boldsymbol{f}(t,\boldsymbol{x}_i(t))=(f_1(t,\boldsymbol{x}_i(t)),\cdots,f_n(t,\boldsymbol{x}_i(t)))^{\mathrm{T}}$为系统的非线性复向量.

同时，第q个领导者的方程为

$$\left.\begin{aligned}\dot{\boldsymbol{x}}_q(t)&=\boldsymbol{A}\boldsymbol{x}_q(t)+\boldsymbol{f}(t,\boldsymbol{x}_q(t)),\\ \boldsymbol{y}_q(t)&=\boldsymbol{C}\boldsymbol{x}_q(t).\end{aligned}\right\}\tag{2}$$

其中：$q\in\{N+1,\cdots,N+M\}$；$\boldsymbol{x}_q(t)\in\boldsymbol{C}^n$表示领导者的复值状态向量；$\boldsymbol{f}(t,\boldsymbol{x}_q(t))$为领导者方程中的复值非线性向量.

此外，本文采用下列3个必要的假设：

假设1[4] 矩阵对$(\boldsymbol{A},\boldsymbol{B})$是可控的；

假设2[4] 矩阵对$(\boldsymbol{A},\boldsymbol{C})$是可观测的；

假设3[4] 对于任意$\boldsymbol{\psi},\boldsymbol{\omega}_m\in\boldsymbol{C}^n$，存在正常数$l$和$\eta_1,\eta_2,\cdots,\eta_M$，且$\sum_{m=1}^{M}\eta_m=1$，使得$\|\boldsymbol{f}(t,\boldsymbol{\psi})-\sum_{m=1}^{M}\eta_m\boldsymbol{f}(t,\boldsymbol{\omega}_m)\|\leqslant l\|\boldsymbol{\psi}-\sum_{m=1}^{M}\eta_m\boldsymbol{\omega}_m\|$.

1.2 时滞攻击

现代网络物理系统依赖可靠的信道来完成协作任务. 本文研究一类改变信道时间特征的网络攻击，即时滞攻击(TDA). 攻击者可以通过网络链路延迟传感器和控制器之间的通信，以阻止控制器及时接收跟随者状态信息，这种攻击可以在多智能体系统的测量通道中发起. 因此，此类攻击会导致某些网络节点接收到的信号延迟甚至无法接收到信号.

本文所考虑的时滞攻击如图1所示.

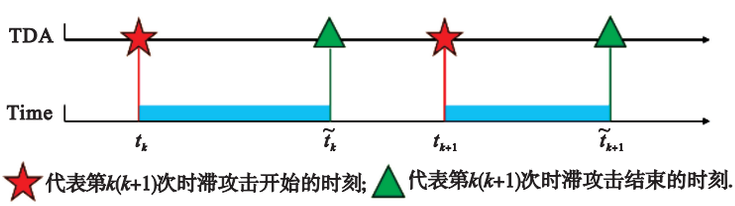


图1 时滞攻击下不同场景的时间轴

Fig. 1 Timeline of different scenarios of time-delay attack

基于图1，定义$[t_0,t_\infty)$内时滞攻击总区间为$\Delta_a^{\mathrm{t}}(t_0,t_\infty)=\left[\bigcup_{k\in N_+}[t_k,\tilde{t}_k)\right]\bigcap[t_0,t_\infty)$. 相应地，再定义$[t_0,t_\infty)$内系统正常运行的总区间为$\Delta_s^{\mathrm{t}}(t_0,t_\infty)=[t_0,t_\infty)\backslash\Delta_a^{\mathrm{t}}(t_0,t_\infty)$. 时滞攻击下跟随者的补偿输出$\boldsymbol{y}_i^{\mathrm{c}}(t)$可以表示为

$$\boldsymbol{y}_i^{\mathrm{c}}(t)=\begin{cases}\boldsymbol{y}_i(t), & t\in\Delta_s^{\mathrm{t}}(t_0,t_\infty),\\ \boldsymbol{y}_i(t-\tau_k), & t\in\Delta_a^{\mathrm{t}}(t_0,t_\infty).\end{cases}\tag{3}$$

其中：时滞$\tau_k\in(0,\tau]$，τ为1个正常数，表示时滞的上界.

1.3 目标阐述与控制方案设计

定义1[7] 如果对于任意$x,y\in D$和任意$\lambda\in[0,1]$，都有$(1-\lambda)x+\lambda y\in D$，则集合$D\subseteq\mathbf{R}^n$为凸集. 若$Co(X)=\left\{\sum_{r=1}^{q}\alpha_r x_r\,|\,x_r\in X,\alpha_r\geqslant 0,\sum_{r=1}^{q}\alpha_r=1\right\}$，则称有限点集$X=\{x_1,x_2,\cdots,x_q\}$的凸包$Co(X)$是包含$X$中所有点的最小凸集.

定义2[7] 对于有M个领导者和N个跟随者的多智能体系统，如果所有跟随者的测量输出最终可以收敛到领导者输出所形成的凸包内，即$\lim_{t\to\infty}\mathrm{dist}\left(\boldsymbol{y}_i(t),Co(\bar{\boldsymbol{y}}(t))\right)=0$. 其中，$\bar{\boldsymbol{y}}(t)=\left(\boldsymbol{y}_{N+1}^{\mathrm{T}},\boldsymbol{y}_{N+2}^{\mathrm{T}},\cdots,\boldsymbol{y}_{N+M}^{\mathrm{T}}\right)^{\mathrm{T}}$，则称系统实现输出包围控制.

本研究旨在构建弹性控制协议，使受攻击的多智能体系统能够实现输出包围一致性. 受实际约束与成本限制，难以对所有智能体状态进

行直接测量,为此构建了针对跟随者的状态观测器:

$$\left.\begin{aligned}&\dot{\hat{\boldsymbol{x}}}_i(t)=\boldsymbol{A}\hat{\boldsymbol{x}}_i(t)+\boldsymbol{B}\boldsymbol{u}_i(t)+\boldsymbol{f}(t,\hat{\boldsymbol{x}}_i(t))+\boldsymbol{J}_s(\boldsymbol{y}_i^{\mathrm{c}}(t)-\hat{\boldsymbol{y}}_i(t)),\\&\hat{\boldsymbol{y}}_i(t)=\boldsymbol{C}\hat{\boldsymbol{x}}_i(t).\end{aligned}\right\}\tag{4}$$

其中:$\hat{\boldsymbol{x}}_i(t)\in\boldsymbol{C}^n$,$\hat{\boldsymbol{y}}_i(t)\in\boldsymbol{C}^m$ 分别为观测器的状态和输出;$\boldsymbol{y}_i^{\mathrm{c}}(t)$ 为补偿输出;观测器增益矩阵 $\boldsymbol{J}_s\in\boldsymbol{C}^{n\times m}$,$s=1,2$,将在后续进行设计.

因此,本文目标可表示为

(i) $\lim\limits_{t\to+\infty}\left(\hat{\boldsymbol{x}}_i(t)-\boldsymbol{x}_i(t)\right)=0$,

(ii) $\lim\limits_{t\to+\infty}\left(\boldsymbol{y}_i(t)-\sum\limits_{q=N+1}^{N+M}l_{iq}\boldsymbol{y}_q(t)\right)=0$.

其中,$\sum\limits_{q=N+1}^{N+M}l_{iq}=1$.

注释1　由于实践中几乎不可能产生无界攻击信号,因此 $\boldsymbol{y}_i(t-\tau_k)$ 为有界信号,又因为 $\hat{\boldsymbol{y}}_i(t)$ 也有界,则存在常数 $d>0$,满足

$$\left\|\boldsymbol{y}(t-\tau_k)-\hat{\boldsymbol{y}}(t)\right\|_2\leqslant d.$$

为了实现输出包围控制,本文考虑采用以下分布式切换控制协议:

$$\begin{aligned}\boldsymbol{u}_i(t)=-\mu\boldsymbol{K}_s\Bigg[&\sum_{j=1}^{N}a_{ij}\left(\hat{\boldsymbol{x}}_i(t)-\hat{\boldsymbol{x}}_j(t)\right)+\\&\sum_{q=N+1}^{N+M}a_{iq}\left(\hat{\boldsymbol{x}}_i(t)-\boldsymbol{x}_q(t)\right)\Bigg]+\boldsymbol{Q}_s(\boldsymbol{y}_i^{\mathrm{c}}(t)-\hat{\boldsymbol{y}}_i(t)).\end{aligned}\tag{5}$$

其中:$\mu>0$ 表示耦合强度;$\boldsymbol{K}_s\in\boldsymbol{C}^{p\times n}$ 表示常数增益矩阵;$\boldsymbol{Q}_s=\begin{cases}\boldsymbol{0}, & s=1,\\ \boldsymbol{J}_2, & s=2.\end{cases}$

为方便表达,令 $\boldsymbol{x}(t)$,$\bar{\boldsymbol{x}}(t)$ 和 $\hat{\boldsymbol{x}}(t)$ 分别为全体跟随者、领导者以及观测器的状态列向量,$\boldsymbol{x}(t)=(\boldsymbol{x}_1^{\mathrm{T}}(t),\cdots,\boldsymbol{x}_N^{\mathrm{T}}(t))^{\mathrm{T}}$,$\bar{\boldsymbol{x}}(t)=(\boldsymbol{x}_{N+1}^{\mathrm{T}}(t),\cdots,\boldsymbol{x}_{N+M}^{\mathrm{T}}(t))^{\mathrm{T}}$,$\hat{\boldsymbol{x}}(t)=(\hat{\boldsymbol{x}}_1^{\mathrm{T}}(t),\cdots,\hat{\boldsymbol{x}}_N^{\mathrm{T}}(t))^{\mathrm{T}}$. 令 $\boldsymbol{y}(t)$,$\bar{\boldsymbol{y}}(t)$ 和 $\hat{\boldsymbol{y}}(t)$ 分别为全体跟随者、领导者和观测器输出列向量:$\boldsymbol{y}(t)=(\boldsymbol{y}_1^{\mathrm{T}}(t),\cdots,\boldsymbol{y}_N^{\mathrm{T}}(t))^{\mathrm{T}}$,$\bar{\boldsymbol{y}}(t)=(\boldsymbol{y}_{N+1}^{\mathrm{T}}(t),\cdots,\boldsymbol{y}_{N+M}^{\mathrm{T}}(t))^{\mathrm{T}}$,$\hat{\boldsymbol{y}}(t)=(\hat{\boldsymbol{y}}_1^{\mathrm{T}}(t),\cdots,\hat{\boldsymbol{y}}_N^{\mathrm{T}}(t))^{\mathrm{T}}$. 同时,跟随者的补偿输出和非线性列向量可表示为 $\boldsymbol{y}(t-\tau_k)=(\boldsymbol{y}_1^{\mathrm{T}}(t-\tau_k),\cdots,\boldsymbol{y}_N^{\mathrm{T}}(t-\tau_k))^{\mathrm{T}}$,$\boldsymbol{F}(t,\boldsymbol{x}(t))=\left(\boldsymbol{f}^{\mathrm{T}}(t,\boldsymbol{x}_1(t)),\cdots,\boldsymbol{f}^{\mathrm{T}}(t,\boldsymbol{x}_N(t))\right)^{\mathrm{T}}$,$\boldsymbol{F}(t,\hat{\boldsymbol{x}}(t))=\left(\boldsymbol{f}^{\mathrm{T}}(t,\hat{\boldsymbol{x}}_1(t)),\cdots,\boldsymbol{f}^{\mathrm{T}}(t,\hat{\boldsymbol{x}}_N(t))\right)^{\mathrm{T}}$,$\boldsymbol{F}(t,\bar{\boldsymbol{x}}(t))=\left(\boldsymbol{f}^{\mathrm{T}}(t,\boldsymbol{x}_{N+1}(t)),\cdots,\boldsymbol{f}^{\mathrm{T}}(t,\boldsymbol{x}_{N+M}(t))\right)^{\mathrm{T}}$,$\boldsymbol{F}(t,\boldsymbol{r}(t))=\boldsymbol{F}(t,\hat{\boldsymbol{x}}(t))-\boldsymbol{F}(t,\boldsymbol{x}(t))$.

同时,记 $\boldsymbol{u}(t)=(\boldsymbol{u}_1^{\mathrm{T}}(t),\cdots,\boldsymbol{u}_N^{\mathrm{T}}(t))^{\mathrm{T}}$.

基于此,跟随者、领导者和观测器的系统方程描述为

$$\left.\begin{aligned}&\dot{\boldsymbol{x}}(t)=(\boldsymbol{I}_N\otimes\boldsymbol{A})\boldsymbol{x}(t)+(\boldsymbol{I}_N\otimes\boldsymbol{B})\boldsymbol{u}(t)+\boldsymbol{F}(t,\boldsymbol{x}(t)),\\&\boldsymbol{y}(t)=(\boldsymbol{I}_N\otimes\boldsymbol{C})\boldsymbol{x}(t);\end{aligned}\right\}\tag{6}$$

$$\left.\begin{aligned}&\dot{\bar{\boldsymbol{x}}}(t)=(\boldsymbol{I}_M\otimes\boldsymbol{A})\bar{\boldsymbol{x}}(t)+\boldsymbol{F}(t,\bar{\boldsymbol{x}}(t)),\\&\bar{\boldsymbol{y}}(t)=(\boldsymbol{I}_M\otimes\boldsymbol{C})\bar{\boldsymbol{x}}(t);\end{aligned}\right\}\tag{7}$$

$$\left.\begin{aligned}&\dot{\hat{\boldsymbol{x}}}(t)=(\boldsymbol{I}_N\otimes\boldsymbol{A})\hat{\boldsymbol{x}}(t)+(\boldsymbol{I}_N\otimes\boldsymbol{B})\boldsymbol{u}(t)+\boldsymbol{F}(t,\hat{\boldsymbol{x}}(t))+\\&\qquad(\boldsymbol{I}_N\otimes\boldsymbol{J}_s)(\boldsymbol{y}^{\mathrm{c}}(t)-\hat{\boldsymbol{y}}(t)),\\&\hat{\boldsymbol{y}}(t)=(\boldsymbol{I}_N\otimes\boldsymbol{C})\hat{\boldsymbol{x}}(t).\end{aligned}\right\}\tag{8}$$

定义状态估计误差 $\boldsymbol{r}(t)=\hat{\boldsymbol{x}}(t)-\boldsymbol{x}(t)$,其中 $\boldsymbol{r}(t)=\left(\boldsymbol{r}_1^{\mathrm{T}}(t),\cdots,\boldsymbol{r}_N^{\mathrm{T}}(t)\right)^{\mathrm{T}}$,$\boldsymbol{r}_i(t)=\hat{\boldsymbol{x}}_i(t)-\boldsymbol{x}_i(t)$. 同时,定义状态包围误差 $\boldsymbol{\zeta}(t)=\boldsymbol{x}(t)-(-\boldsymbol{L}_1^{-1}\boldsymbol{L}_2\otimes\boldsymbol{I}_n)\bar{\boldsymbol{x}}(t)$,其中 $\boldsymbol{\zeta}(t)=(\boldsymbol{\zeta}_1^{\mathrm{T}}(t),\cdots,\boldsymbol{\zeta}_N^{\mathrm{T}}(t))^{\mathrm{T}}$,$\boldsymbol{\zeta}_i(t)=\boldsymbol{x}_i(t)-\sum\limits_{q=N+1}^{N+M}l_{iq}\boldsymbol{x}_q(t)$. 定义输出包围误差 $\boldsymbol{e}(t)=\boldsymbol{y}(t)-(-\boldsymbol{L}_1^{-1}\boldsymbol{L}_2\otimes\boldsymbol{I}_m)\bar{\boldsymbol{y}}(t)$,其中 $\boldsymbol{e}(t)=(\boldsymbol{e}_1^{\mathrm{T}}(t),\cdots,\boldsymbol{e}_N^{\mathrm{T}}(t))^{\mathrm{T}}$,$\boldsymbol{e}_i(t)=\boldsymbol{y}_i(t)-\sum\limits_{q=N+1}^{N+M}l_{iq}\boldsymbol{y}_q(t)$.

结合式(6)和式(8),状态估计误差 $\boldsymbol{r}(t)$ 的切换动态方程为

$$\dot{\boldsymbol{r}}(t)=\begin{cases}\left[\boldsymbol{I}_N\otimes(\boldsymbol{A}+\boldsymbol{J}_1\boldsymbol{C})\right]\boldsymbol{r}(t)+\boldsymbol{F}(t,\boldsymbol{r}(t)), & t\in\Delta_s^{\mathrm{t}}(t_0,t_\infty),\\(\boldsymbol{I}_N\otimes\boldsymbol{A})\boldsymbol{r}(t)+\boldsymbol{F}(t,\boldsymbol{r}(t))+ & \\(\boldsymbol{I}_N\otimes\boldsymbol{J}_2)(\boldsymbol{y}(t-\tau_k)-\hat{\boldsymbol{y}}(t)), & t\in\Delta_a^{\mathrm{t}}(t_0,t_\infty).\end{cases}\tag{9}$$

类似地,结合式(6)和式(7),可以得到状态包围误差 $\boldsymbol{\zeta}(t)$ 的切换动态方程为

$$\dot{\boldsymbol{\zeta}}(t)=\begin{cases}\left(\boldsymbol{I}_N\otimes\boldsymbol{A}\right)\boldsymbol{\zeta}(t)+\boldsymbol{F}(t,\boldsymbol{x}(t))+\left(\boldsymbol{L}_1^{-1}\boldsymbol{L}_2\otimes\boldsymbol{I}_n\right)\boldsymbol{F}(t,\bar{\boldsymbol{x}}(t))-\mu\left(\boldsymbol{L}_1\otimes\boldsymbol{B}\boldsymbol{K}_1\right)\boldsymbol{\zeta}(t)+\mu\left(\boldsymbol{L}_1\otimes\boldsymbol{B}\boldsymbol{K}_1\right)\boldsymbol{r}(t), & t\in\Delta_s^{\mathrm{t}}(t_0,t_\infty),\\\left(\boldsymbol{I}_N\otimes\boldsymbol{A}\right)\boldsymbol{\zeta}(t)+\boldsymbol{F}(t,\boldsymbol{x}(t))+\left(\boldsymbol{L}_1^{-1}\boldsymbol{L}_2\otimes\boldsymbol{I}_n\right)\boldsymbol{F}(t,\bar{\boldsymbol{x}}(t))-\mu\left(\boldsymbol{L}_1\otimes\boldsymbol{B}\boldsymbol{K}_2\right)\boldsymbol{\zeta}(t)+\mu\left(\boldsymbol{L}_1\otimes\boldsymbol{B}\boldsymbol{K}_2\right)\boldsymbol{r}(t)+ & \\\left(\boldsymbol{I}_N\otimes\boldsymbol{B}\boldsymbol{J}_2\right)\left(\boldsymbol{y}(t-\tau_k)-\hat{\boldsymbol{y}}(t)\right), & t\in\Delta_a^{\mathrm{t}}(t_0,t_\infty).\end{cases}\tag{10}$$

综上所述,本文目标可进一步转化为保证复值误差系统的稳定性,即 $\lim\limits_{t\to\infty}\|\boldsymbol{r}(t)\|=0$ 且 $\lim\limits_{t\to\infty}\|\boldsymbol{\zeta}(t)\|=0$.

1.4　预备知识

假设4[4]　对于任意跟随者,当 $t\in\Delta_s^{\mathrm{t}}(t_0,t_\infty)$ 时,至少存在1个具有到它定向路径的领导者.

定义3[4]　令 $[t_k,\tilde{t}_k)$ 和 $[\tilde{t}_k,t_{k+1})$ 分别为第 k 次攻击期和休眠期. 同时,对于时滞攻击,定义 $\Upsilon=\limsup\limits_{k\to+\infty}\dfrac{\tilde{t}_{k+1}-t_{k+1}}{\tilde{t}_{k+1}-\tilde{t}_k},k\in\mathbf{N}_+$.

注释2　根据定义3,显然,$0<\Upsilon<1$.

假设5[4]　攻击检测装置会立即检测到相关

的网络攻击,并且设置中不可能出现检测错误.

引理 1[4] 令矩阵 $\boldsymbol{A}=\begin{bmatrix}-ab\boldsymbol{I}_{Mn} & ac\boldsymbol{B}\\ ac\boldsymbol{B}^{H} & -b\boldsymbol{I}_{Mn}\end{bmatrix}$ 为 1 个 Hermite 矩阵,其中 $\boldsymbol{B}\in\boldsymbol{C}^{Mn\times Mn}$ 且 a,b,c 均为正常数.如果 a 是一个足够小的正数,则矩阵 $\boldsymbol{A}$ 为负定矩阵.

引理 2[12] $\Gamma(t)$ 对于 $t\in[0,+\infty)$ 是非负连续函数,并满足以下条件:

$$\dot{\Gamma}(t)\leqslant\begin{cases}-\rho_1\Gamma(t), & t\in\Delta_s^{\mathrm{t}}(t_0,t_\infty),\\ \rho_2\Gamma(t), & t\in\Delta_a^{\mathrm{t}}(t_0,t_\infty),\end{cases}$$

其中 ρ_1,ρ_2 均为常数,如果 $\rho_1>0$,$\chi=\rho_1(1-\Upsilon)-\rho_2\Upsilon>0$,那么 $\Gamma(t)\leqslant\Gamma(0)\exp\{-\chi t\}$,$t\geqslant 0$.

2 主要结果

本章得到了跟随者(1)和领导者(2)在时滞攻击下的输出包围一致性,考虑了系统 2 种不同情况:无时滞攻击下系统正常期和时滞攻击下系统攻击期,从而给出关于输出包围控制的结果.

定理 1 在假设 1~5 下,若存在矩阵 $\boldsymbol{K}_1,\boldsymbol{K}_2$ 和 $\boldsymbol{J}_1,\boldsymbol{J}_2$,标量 ρ_1,ρ_2,$0<\Upsilon<1$ 以及正常数 $\varepsilon_1,\varepsilon_2,\varepsilon_3,\varepsilon_4$,使得

$$\rho_1<-\max\{\delta_1,\delta_2\},\rho_2>\max\{\delta_3,\delta_4\}. \tag{11}$$

其中:$\delta_1=\lambda_{\max}\left[\boldsymbol{I}_N\otimes\left(\boldsymbol{A}+\boldsymbol{J}_1\boldsymbol{C}\right)\right]^{\mathrm{S}}+\varepsilon_1+\dfrac{l^2}{\varepsilon_1}$;

$\delta_2=\lambda_{\max}\left[\left(\boldsymbol{I}_N\otimes\boldsymbol{A}\right)-\mu\left(\boldsymbol{L}_1\otimes\boldsymbol{B}\boldsymbol{K}_1\right)\right]^{\mathrm{S}}+\varepsilon_2+\dfrac{l^2}{\varepsilon_2}$;

$\delta_3=\lambda_{\max}\left(\boldsymbol{I}_N\otimes\boldsymbol{A}\right)^{\mathrm{S}}+\varepsilon_3+\dfrac{l^2}{\varepsilon_3}$;$\delta_4=\lambda_{\max}\left[\left(\boldsymbol{I}_N\otimes\boldsymbol{A}\right)-\mu\left(\boldsymbol{L}_1\otimes\boldsymbol{B}\boldsymbol{K}_2\right)\right]^{\mathrm{S}}+\varepsilon_4+\dfrac{l^2}{\varepsilon_4}$.跟随者(1)和领导者(2)通过观测器(4)和分布式切换控制协议(5)能够实现时滞攻击下输出包围控制.

证明 构造如下形式的 Lyapunov 函数:

$$V(t)=\theta\left(V_1(t)+V_2(t)\right). \tag{12}$$

其中:$V_1(t)=\boldsymbol{r}^{\mathrm{H}}(t)\boldsymbol{r}(t)$;$V_2(t)=\boldsymbol{\zeta}^{\mathrm{H}}(t)\boldsymbol{\zeta}(t)$;$\theta$ 为充分小的正常数.

情况 1 考虑当 $t\in\Delta_s^{\mathrm{t}}(t_0,t_\infty)$ 时,多智能体系统的包围控制情况.

$V_1(t)$ 沿误差系统(9)关于时间 t 的导数为

$$\begin{aligned}\dot{V}_1(t)&=\dot{\boldsymbol{r}}^{\mathrm{H}}(t)\boldsymbol{r}(t)+\boldsymbol{r}^{\mathrm{H}}(t)\dot{\boldsymbol{r}}(t)=\\ &\boldsymbol{r}^{\mathrm{H}}(t)\left[\boldsymbol{I}_N\otimes\left(\boldsymbol{A}+\boldsymbol{J}_1\boldsymbol{C}\right)\right]^{\mathrm{H}}\boldsymbol{r}(t)+\boldsymbol{F}^{\mathrm{H}}(t,\boldsymbol{r}(t))\boldsymbol{r}(t)+\\ &\boldsymbol{r}^{\mathrm{H}}(t)\left[\boldsymbol{I}_N\otimes\left(\boldsymbol{A}+\boldsymbol{J}_1\boldsymbol{C}\right)\right]\boldsymbol{r}(t)+\boldsymbol{r}^{\mathrm{H}}(t)\boldsymbol{F}(t,\boldsymbol{r}(t))=\\ &\boldsymbol{r}^{\mathrm{H}}(t)\left[\boldsymbol{I}_N\otimes\left(\boldsymbol{A}+\boldsymbol{J}_1\boldsymbol{C}\right)\right]^{\mathrm{S}}\boldsymbol{r}(t)+\\ &\boldsymbol{F}^{\mathrm{H}}(t,\boldsymbol{r}(t))\boldsymbol{r}(t)+\boldsymbol{r}^{\mathrm{H}}(t)\boldsymbol{F}(t,\boldsymbol{r}(t)).\end{aligned} \tag{13}$$

随后,对式(13)进行放缩处理,可得

$$\begin{aligned}&\boldsymbol{r}^{\mathrm{H}}(t)\left[\boldsymbol{I}_N\otimes\left(\boldsymbol{A}+\boldsymbol{J}_1\boldsymbol{C}\right)\right]^{\mathrm{S}}\boldsymbol{r}(t)\leqslant\\ &\lambda_{\max}\left[\boldsymbol{I}_N\otimes\left(\boldsymbol{A}+\boldsymbol{J}_1\boldsymbol{C}\right)\right]^{\mathrm{S}}\boldsymbol{r}^{\mathrm{H}}(t)\boldsymbol{r}(t),\\ &\boldsymbol{F}^{\mathrm{H}}(t,\boldsymbol{r}(t))\boldsymbol{r}(t)+\boldsymbol{r}^{\mathrm{H}}(t)\boldsymbol{F}(t,\boldsymbol{r}(t))\leqslant\varepsilon_1\boldsymbol{r}^{\mathrm{H}}(t)\boldsymbol{r}(t)+\\ &\frac{1}{\varepsilon_1}\boldsymbol{F}^{\mathrm{H}}(t,\boldsymbol{r}(t))\boldsymbol{F}(t,\boldsymbol{r}(t))\leqslant\varepsilon_1\boldsymbol{r}^{\mathrm{H}}(t)\boldsymbol{r}(t)+\frac{l^2}{\varepsilon_1}\boldsymbol{r}^{\mathrm{H}}(t)\boldsymbol{r}(t).\end{aligned} \tag{14}$$

因此,式(13)可放缩为 $\dot{V}_1(t)\leqslant\delta_1V_1(t)$.

同时,$V_2(t)$ 沿误差系统(10)关于时间 t 的导数为

$$\begin{aligned}\dot{V}_2(t)=&\dot{\boldsymbol{\zeta}}^{\mathrm{H}}(t)\boldsymbol{\zeta}(t)+\boldsymbol{\zeta}^{\mathrm{H}}(t)\dot{\boldsymbol{\zeta}}(t)=\boldsymbol{\zeta}^{\mathrm{H}}(t)\left(\boldsymbol{I}_N\otimes\boldsymbol{A}\right)^{\mathrm{H}}\boldsymbol{\zeta}(t)+\boldsymbol{F}^{\mathrm{H}}(t,\boldsymbol{x}(t))\boldsymbol{\zeta}(t)+\boldsymbol{F}^{\mathrm{H}}(t,\bar{\boldsymbol{x}}(t))\left(\boldsymbol{L}_1^{-1}\boldsymbol{L}_2\otimes\boldsymbol{I}_n\right)^{\mathrm{H}}\boldsymbol{\zeta}(t)-\\ &\mu\boldsymbol{\zeta}^{\mathrm{H}}(t)\left(\boldsymbol{L}_1\otimes\boldsymbol{B}\boldsymbol{K}_1\right)^{\mathrm{H}}\boldsymbol{\zeta}(t)+\mu\boldsymbol{r}^{\mathrm{H}}(t)\left(\boldsymbol{L}_1\otimes\boldsymbol{B}\boldsymbol{K}_1\right)^{\mathrm{H}}\boldsymbol{\zeta}(t)+\boldsymbol{\zeta}^{\mathrm{H}}(t)\left(\boldsymbol{I}_N\otimes\boldsymbol{A}\right)\boldsymbol{\zeta}(t)+\boldsymbol{\zeta}^{\mathrm{H}}(t)\boldsymbol{F}(t,\boldsymbol{x}(t))+\\ &\boldsymbol{\zeta}^{\mathrm{H}}(t)\left(\boldsymbol{L}_1^{-1}\boldsymbol{L}_2\otimes\boldsymbol{I}_n\right)\boldsymbol{F}(t,\bar{\boldsymbol{x}}(t))-\mu\boldsymbol{\zeta}^{\mathrm{H}}(t)\left(\boldsymbol{L}_1\otimes\boldsymbol{B}\boldsymbol{K}_1\right)\boldsymbol{\zeta}(t)+\mu\boldsymbol{\zeta}^{\mathrm{H}}(t)\left(\boldsymbol{L}_1\otimes\boldsymbol{B}\boldsymbol{K}_1\right)\boldsymbol{r}(t).\end{aligned} \tag{15}$$

类似地,式(15)可放缩为

$$\begin{aligned}\dot{V}_2(t)\leqslant&\delta_2V_2(t)+\mu\boldsymbol{r}^{\mathrm{H}}(t)\left(\boldsymbol{L}_1\otimes\boldsymbol{B}\boldsymbol{K}_1\right)^{\mathrm{H}}\boldsymbol{\zeta}(t)+\\ &\mu\boldsymbol{\zeta}^{\mathrm{H}}(t)\left(\boldsymbol{L}_1\otimes\boldsymbol{B}\boldsymbol{K}_1\right)\boldsymbol{r}(t).\end{aligned} \tag{16}$$

取 $-\rho_1>\max\{\delta_1,\delta_2\}$,从而得到

$$\begin{aligned}\dot{V}(t)\leqslant&-\rho_1V(t)+\theta\mu\boldsymbol{r}^{\mathrm{H}}(t)\left(\boldsymbol{L}_1\otimes\boldsymbol{B}\boldsymbol{K}_1\right)^{\mathrm{H}}\boldsymbol{\zeta}(t)+\\ &\theta\mu\boldsymbol{\zeta}^{\mathrm{H}}(t)\left(\boldsymbol{L}_1\otimes\boldsymbol{B}\boldsymbol{K}_1\right)\boldsymbol{r}(t).\end{aligned} \tag{17}$$

令 $\boldsymbol{E}_1(t)=\left(\boldsymbol{\zeta}^{\mathrm{H}}(t),\boldsymbol{r}^{\mathrm{H}}(t)\right)^{\mathrm{H}}$,以及矩阵 $\boldsymbol{\Omega}_1=\begin{bmatrix}\boldsymbol{0} & \theta\mu\left(\boldsymbol{L}_1\otimes\boldsymbol{B}\boldsymbol{K}_1\right)\\ \theta\mu\left(\boldsymbol{L}_1\otimes\boldsymbol{B}\boldsymbol{K}_1\right)^{\mathrm{H}} & \boldsymbol{0}\end{bmatrix}$,可得

$$\dot{V}(t)\leqslant-\rho_1V(t)+\boldsymbol{E}_1^{\mathrm{H}}(t)\boldsymbol{\Omega}_1\boldsymbol{E}_1(t), \tag{18}$$

则一定存在常数 $\tilde{\rho}_1$,满足 $0<\tilde{\rho}_1<<\rho_1$,使得

$$\begin{aligned}\dot{V}(t)<&-\rho_1V(t)+\boldsymbol{E}_1^{\mathrm{H}}(t)\boldsymbol{\Omega}_1\boldsymbol{E}_1(t)-\tilde{\rho}_1V_1(t)-\\ &\tilde{\rho}_1\theta V_2(t)=-\rho_1V(t)+\boldsymbol{E}_1^{\mathrm{H}}(t)\boldsymbol{\Omega}_2\boldsymbol{E}_1(t).\end{aligned} \tag{19}$$

其中,$\boldsymbol{\Omega}_2=\begin{bmatrix}-\theta\tilde{\rho}_1\left(\boldsymbol{I}_N\otimes\boldsymbol{I}_n\right) & \theta\mu\left(\boldsymbol{L}_1\otimes\boldsymbol{B}\boldsymbol{K}_1\right)\\ \theta\mu\left(\boldsymbol{L}_1\otimes\boldsymbol{B}\boldsymbol{K}_1\right)^{\mathrm{H}} & -\tilde{\rho}_1\left(\boldsymbol{I}_N\otimes\boldsymbol{I}_n\right)\end{bmatrix}$.

根据引理 1,则存在充分小的常数 $\theta>0$,使得矩阵 $\boldsymbol{\Omega}_2$ 为负定矩阵,所以

$$\dot{V}(t)<-\rho_1V(t). \tag{20}$$

情况 2 考虑当 $t\in\Delta_a^{\mathrm{t}}(t_0,t_\infty)$ 时,多智能体系

统的包围控制情况.

在此情况下,$V_1(t)$沿误差系统(9)关于时间t的导数满足

$$\dot{V}_1(t)\leqslant\delta_3 V_1(t)+\left(\boldsymbol{y}(t-\tau_k)-\hat{\boldsymbol{y}}(t)\right)^{\mathrm{H}}\left(\boldsymbol{I}_N\otimes\boldsymbol{J}_2\right)^{\mathrm{H}}\boldsymbol{r}(t)+\boldsymbol{r}^{\mathrm{H}}(t)\left(\boldsymbol{I}_N\otimes\boldsymbol{J}_2\right)\left(\boldsymbol{y}(t-\tau_k)-\hat{\boldsymbol{y}}(t)\right).\tag{21}$$

类似地,$V_2(t)$沿误差系统(10)关于时间t的导数满足

$$\dot{V}_2(t)\leqslant\delta_4 V_2(t)+\left(\boldsymbol{y}(t-\tau_k)-\hat{\boldsymbol{y}}(t)\right)^{\mathrm{H}}\left(\boldsymbol{I}_N\otimes\boldsymbol{B}\boldsymbol{J}_2\right)^{\mathrm{H}}\boldsymbol{\zeta}(t)+\boldsymbol{\zeta}^{\mathrm{H}}(t)\left(\boldsymbol{I}_N\otimes\boldsymbol{B}\boldsymbol{J}_2\right)\left(\boldsymbol{y}(t-\tau_k)-\hat{\boldsymbol{y}}(t)\right)+\mu\boldsymbol{r}^{\mathrm{H}}(t)\cdot\left(\boldsymbol{L}_1\otimes\boldsymbol{B}\boldsymbol{K}_2\right)^{\mathrm{H}}\boldsymbol{\zeta}(t)+\mu\boldsymbol{\zeta}^{\mathrm{H}}(t)\left(\boldsymbol{L}_1\otimes\boldsymbol{B}\boldsymbol{K}_2\right)\boldsymbol{r}(t).\tag{22}$$

取常数$\rho_2>\max\{\delta_3,\delta_4\}$,与此同时,再令$\tilde{\boldsymbol{y}}(t)=\boldsymbol{y}(t-\tau_k)-\hat{\boldsymbol{y}}(t)$,可得

$$\dot{V}(t)\leqslant\rho_2 V(t)+\theta\tilde{\boldsymbol{y}}^{\mathrm{H}}(t)\left(\boldsymbol{I}_N\otimes\boldsymbol{J}_2\right)^{\mathrm{H}}\boldsymbol{r}(t)+\theta\boldsymbol{r}^{\mathrm{H}}(t)\left(\boldsymbol{I}_N\otimes\boldsymbol{J}_2\right)\tilde{\boldsymbol{y}}(t)+\theta\tilde{\boldsymbol{y}}^{\mathrm{H}}(t)\left(\boldsymbol{I}_N\otimes\boldsymbol{B}\boldsymbol{J}_2\right)^{\mathrm{H}}\boldsymbol{\zeta}(t)+\theta\boldsymbol{\zeta}^{\mathrm{H}}(t)\left(\boldsymbol{I}_N\otimes\boldsymbol{B}\boldsymbol{J}_2\right)\cdot\tilde{\boldsymbol{y}}(t)+\theta\mu\boldsymbol{r}^{\mathrm{H}}(t)\left(\boldsymbol{L}_1\otimes\boldsymbol{B}\boldsymbol{K}_2\right)^{\mathrm{H}}\boldsymbol{\zeta}(t)+\theta\mu\boldsymbol{\zeta}^{\mathrm{H}}(t)\left(\boldsymbol{L}_1\otimes\boldsymbol{B}\boldsymbol{K}_2\right)\boldsymbol{r}(t).\tag{23}$$

令$\boldsymbol{E}_2(t)=\left(\boldsymbol{r}^{\mathrm{T}}(t),\boldsymbol{\zeta}^{\mathrm{T}}(t),\tilde{\boldsymbol{y}}^{\mathrm{T}}(t),\tilde{\boldsymbol{y}}^{\mathrm{T}}(t)\right)^{\mathrm{T}}$,以及矩阵

$$\boldsymbol{\Omega}_3=\begin{bmatrix}\boldsymbol{0}&\boldsymbol{0}&\boldsymbol{0}&\theta\left(\boldsymbol{I}_N\otimes\boldsymbol{J}_2\right)\\ \boldsymbol{0}&\boldsymbol{0}&\theta\left(\boldsymbol{I}_N\otimes\boldsymbol{B}\boldsymbol{J}_2\right)&\boldsymbol{0}\\ \boldsymbol{0}&\theta\left(\boldsymbol{I}_N\otimes\boldsymbol{B}\boldsymbol{J}_2\right)^{\mathrm{H}}&\boldsymbol{0}&\boldsymbol{0}\\ \theta\left(\boldsymbol{I}_N\otimes\boldsymbol{J}_2\right)^{\mathrm{H}}&\boldsymbol{0}&\boldsymbol{0}&\boldsymbol{0}\end{bmatrix},$$

可得$\dot{V}(t)<\rho_2 V(t)+\boldsymbol{E}_1^{\mathrm{H}}(t)\boldsymbol{\Omega}_1\boldsymbol{E}_1(t)+\boldsymbol{E}_2^{\mathrm{H}}(t)\boldsymbol{\Omega}_3\boldsymbol{E}_2(t)$,因此存在1个充分小的正常数$\tilde{\rho}_2$,满足$0<\tilde{\rho}_2<<|\rho_2|$,从而使得

$$\dot{V}(t)<\rho_2 V(t)+\boldsymbol{E}_1^{\mathrm{H}}(t)\boldsymbol{\Omega}_1\boldsymbol{E}_1(t)+\boldsymbol{E}_2^{\mathrm{H}}(t)\boldsymbol{\Omega}_3\boldsymbol{E}_2(t)-\tilde{\rho}_2\tilde{V}(t)=\rho_2 V(t)+\boldsymbol{E}_1^{\mathrm{H}}(t)\boldsymbol{\Omega}_2\boldsymbol{E}_1(t)+\boldsymbol{E}_2^{\mathrm{H}}(t)\boldsymbol{\Omega}_4\boldsymbol{E}_2(t).\tag{24}$$

其中:$\tilde{V}(t)=V(t)+V_1(t)+\theta V_2(t)+2d$;

$$\boldsymbol{\Omega}_4=\begin{bmatrix}-\theta\tilde{\rho}_2\left(\boldsymbol{I}_N\otimes\boldsymbol{I}_n\right)&\boldsymbol{0}&\boldsymbol{0}&\theta\left(\boldsymbol{I}_N\otimes\boldsymbol{J}_2\right)\\ \boldsymbol{0}&-\theta\tilde{\rho}_2\left(\boldsymbol{I}_N\otimes\boldsymbol{I}_n\right)&\theta\left(\boldsymbol{I}_N\otimes\boldsymbol{B}\boldsymbol{J}_2\right)&\boldsymbol{0}\\ \boldsymbol{0}&\theta\left(\boldsymbol{I}_N\otimes\boldsymbol{B}\boldsymbol{J}_2\right)^{\mathrm{H}}&-\tilde{\rho}_2\left(\boldsymbol{I}_N\otimes\boldsymbol{I}_n\right)&\boldsymbol{0}\\ \theta\left(\boldsymbol{I}_N\otimes\boldsymbol{J}_2\right)^{\mathrm{H}}&\boldsymbol{0}&\boldsymbol{0}&-\tilde{\rho}_2\left(\boldsymbol{I}_N\otimes\boldsymbol{I}_n\right)\end{bmatrix}.$$

结合引理1,则存在充分小的常数$\theta>0$,使得矩阵$\boldsymbol{\Omega}_2,\boldsymbol{\Omega}_4$均为负定矩阵,所以

$$\dot{V}(t)<\rho_2 V(t).\tag{25}$$

根据引理2,$V(t)\leqslant V(0)\exp\{-\chi t\}$,因为$\chi>0$,则当$t\to\infty$时,状态估计误差$\boldsymbol{r}(t)\to 0$,状态包围误差$\boldsymbol{\zeta}(t)\to 0$,则输出包围误差$\boldsymbol{e}(t)=\boldsymbol{C}\boldsymbol{\zeta}(t)\to 0$.这表明多智能体系统中的跟随者(1)和领导者(2)通过观测器(4)和分布式切换控制协议(5)能够实现时滞攻击下输出包围控制.证毕.

注释3　与以往多数针对网络攻击的安全一致性研究不同,本文中的时滞并非来自系统固有特性,而是由攻击行为本身所诱发,且攻击直接作用于系统输出,因而更具工程实用性.进一步,在所提定理中,针对攻击期间状态观测误差及包围误差中的时滞项,通过构造多个与之匹配的高阶负定矩阵进行放缩处理,最终实现状态观测器的精确估计与输出包围的精确控制.

3　数值仿真

考虑1个具有2个领导者和3个跟随者的复值非线性多智能体系统.图2展示了智能体间的有向拓扑通信,其中五边形节点代表领导者,圆形节点代表跟随者.

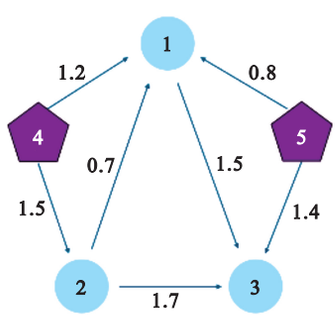


图2　多智能体系统的有向信息拓扑图

Fig. 2　Directed information topology graph of a multi-agent system

每个智能体都由复Lorenz系统描述.在仿真的过程中,选择相应的系统参数为$\boldsymbol{A}=\begin{bmatrix}-5.9 & 5.9 & 0\\ 59+0.19\mathrm{j} & -0.95+0.058\mathrm{j} & 0\\ 0 & 0 & -0.85\end{bmatrix}$,$\boldsymbol{B}=\begin{bmatrix}9&0&0\\0&9&0\\0&0&9\end{bmatrix}$,$\boldsymbol{C}=\begin{bmatrix}0.4&0&0\\0&0.3&-0.25\\0&0&2.4\end{bmatrix}$,在初值$X(0)=(2.05+0.025\mathrm{j},-0.48+0.31\mathrm{j},5.1,1.03+0.032\mathrm{j},-0.21+0.11\mathrm{j},3.05,1.52+0.055\mathrm{j},-0.19+0.61\mathrm{j},4.08)^{\mathrm{T}}$,$\hat{X}(0)=(10.2+2.1\mathrm{j},-5.1+3.05\mathrm{j},15.1,8.1+1.55\mathrm{j},-3.05+2.05\mathrm{j},12.08,12.1+2.55\mathrm{j},-6.05+3.55\mathrm{j},18.1)^{\mathrm{T}}$,$\bar{X}(0)=(5.05+1.55\mathrm{j},-1.02+0.11\mathrm{j},3.22,5.12+1.62\mathrm{j},-1.05+0.13\mathrm{j},3.28)^{\mathrm{T}}$下,未受控制的跟随者(1),领导者(2)和观测器(4)表现出混沌行为,如图3所示,且初值分别对应为$X(0)$,$\bar{X}(0)$和$\hat{X}(0)$.同时,可以计算出$l=60.041\,7$.

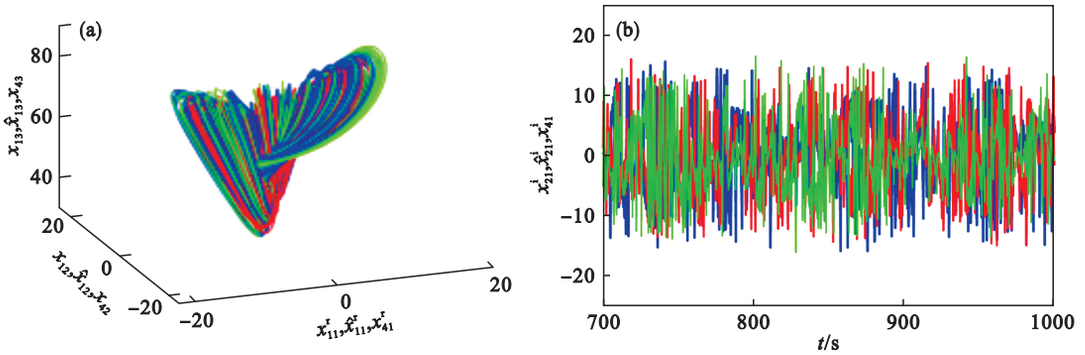


图3 未受控制的跟随者(1)(蓝色),观测器(4)(红色),领导者(2)(绿色)的动力学行为

Fig. 3 Dynamical behaviors of uncontrolled followers (1) (blue), observers (4) (red), and leaders (2) (green)

(a)—混沌吸引子;(b)—状态变量x_{21}^{i},$\hat{x}_{21}^{\mathrm{i}}$,$x_{41}^{\mathrm{i}}$随时间$t$的变化.

为验证控制协议的有效性,选取以下参数值:

$$\mu=13,\boldsymbol{K}_1=\begin{bmatrix}2.54&0&0\\0&5&0\\0&0&11\end{bmatrix},\boldsymbol{K}_2=\begin{bmatrix}3.58&0&0\\0&7&0\\0&0&13\end{bmatrix},$$

$$\boldsymbol{J}_1=\begin{bmatrix}130+12\mathrm{j}&0.12\\0.02&95+21\mathrm{j}\\&0\quad 0\end{bmatrix},\boldsymbol{J}_2=\begin{bmatrix}152+16\mathrm{j}&0.23\\0.27&130+31\mathrm{j}\\&0\quad 0\end{bmatrix}.$$

同时,时滞攻击时间间隔定义为$[0.150\,4,0.150\,8)\cup[0.638\,2,0.638\,6)\cup[1.034\,1,1.034\,7)\cup[1.188,1.195)\cup[1.300,1.305)\cup[1.900,1.907)\cup\cdots$,显然,时滞攻击在1.5 s内发生了5次,且$\Upsilon=0.004\,5$,根据定理1,取$\rho_1=32.4,\rho_2=-27$,符合定理1的条件.此时系统误差动力学如图4所示.状态估计误差和输出包围误差在1.33 s趋近于零,即所提出的控制协议能够实现基于观测器的多智能体系统的输出包围控制.

同时,为展示Υ对系统误差动力学的影响,将攻击频率调整至1.5 s内攻击2次,将时滞攻击的区间调整为$[0.350\,5,0.351)\cup[0.853\,1,0.853\,5)\cup[2.368\,1,2.368\,6)\cup\cdots$,根据定义3,$\Upsilon=0.004\,3$,参数数值保持不变,计算可得定理的条件全部满足.根据图5可知,状态估计误差和输出包围误差在1.31 s时趋近于零,证实了该控制协议在不同时滞攻击频率下是鲁棒的.

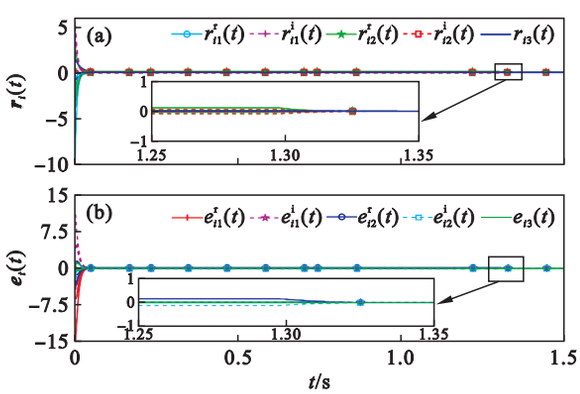


图4 时滞攻击下的误差动力学

Fig. 4 Error dynamics under time-delay attack

(a)—状态估计误差;(b)—输出包围误差,$\Upsilon=0.004\,5$.

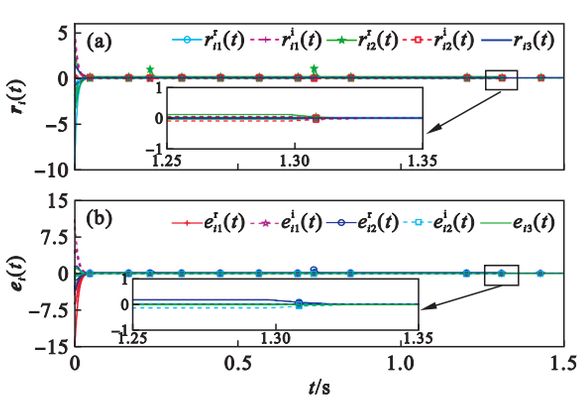


图5 时滞攻击下的误差动力学

Fig. 5 Error dynamics under time-delay attack

(a)—状态估计误差;(b)—输出包围误差,$\Upsilon=0.004\,3$.

4 结　　语

针对复值非线性多智能体系统,本文基于观测器方法研究其输出包围控制问题.将遭受时滞攻击的误差系统建模为切换系统,并利用观测器状态设计分布式切换控制协议,从而保证智能体之间即使存在时滞攻击,仍能实现输出包围一致性.最后,利用数值仿真验证了所提理论方法的有效性.

参考文献:

[1] Ferrari-Trecate G, Egerstedt M, Buffa A, et al. Laplacian sheep: a hybrid, stop-go policy for leader-based containment control[C]// International Workshop on Hybrid Systems: Computation and Control. Berlin, Heidelberg: Springer, 2006: 212-226.

[2] Xiao Q, Lewis F L, Zeng Z G. Containment control for multiagent systems under two intermittent control schemes [J]. *IEEE Transactions on Automatic Control*, 2019, 64(3): 1236-1243.

[3] Wang Q, Dong X W, Yu J L, et al. Predefined finite-time output containment of nonlinear multi-agent systems with leaders of unknown inputs [J]. *IEEE Transactions on Circuits and Systems I: Regular Papers*, 2021, 68(8): 3436-3448.

[4] Liu M X, Liu J, Li H, et al. Secure containment control of time-delay complex-valued multi-agent systems against different attacks[J]. *Nonlinear Dynamics*, 2025, 113(14): 18215-18228.

[5] Liu M X, Liu J, Liang J C, et al. Observer-based secure synchronization control of directed complex-valued dynamical networks under link attacks [J]. *Nonlinear Dynamics*, 2024, 112(14): 12303-12318.

[6] Ma Y S, Che W W, Deng C, et al. Observer-based event-triggered containment control for MASs under DoS attacks [J]. *IEEE Transactions on Cybernetics*, 2022, 52(12): 13156-13167.

[7] Shi Y P, Hu J P, Meng B, et al. Resilient output containment over heterogeneous wide-area networks: mitigating intermittent communication and unknown cyber-attacks [J]. *IEEE Transactions on Circuits and Systems I: Regular Papers*, 2025, 72(5): 2354-2365.

[8] Zhou M, Li H C, Xue T L, et al. Event-triggered state interval estimation and fault-tolerant control for multiagent systems under deception attacks [J]. *IEEE Transactions on Automatic Control*, 2025, 70(1): 689-696.

[9] Pathak P K, Yadav A K, Kamwa I. Robust IMC for time delay attack compensation of renewable supported power system [J]. *IEEE Transactions on Automation Science and Engineering*, 2025, 22: 16532-16546.

[10] Zhai W B, Liu L, Ding Y W, et al. ETD: an efficient time delay attack detection framework for UAV networks [J]. *IEEE Transactions on Information Forensics and Security*, 2023, 18: 2913-2928.

[11] Shen Y, Liu X Z. Leader-follower synchronization of networked multi-agent systems via hybrid protocols [J]. *Asian Journal of Control*, 2024, 26(1): 1-15.

[12] Liu X W, Chen T P. Synchronization of linearly coupled networks with delays via aperiodically intermittent pinning control [J]. *IEEE Transactions on Neural Networks and Learning Systems*, 2015, 26(10): 2396-2407.

(上接第 29 页)

[16] Zhang L S, Li Z J, Peng Y X. A hidden grid multi-scroll chaotic system coined with two multi-stable memristors[J]. *Chaos, Solitons & Fractals*, 2024, 185: 115109.

[17] Huang L L, Chen F Y, Geng F Y, et al. Generation and control of grid multi-vortex attractors in memristive Hopfield neural network[J]. *Chaos, Solitons & Fractals*, 2025, 199: 116717.

[18] Li R H, Dong E Z, Tong J G, et al. A novel multiscroll memristive Hopfield neural network [J]. *International Journal of Bifurcation and Chaos*, 2022, 32(9): 2250130.

[19] Chua L O, Yang L. Cellular neural networks: applications [J]. *IEEE Transactions on Circuits and Systems*, 1988, 35(10): 1273-1290.

[20] Venetianter P L, Roska T. Image compression by cellular neural networks [J]. *Computer Standards & Interfaces*, 1999, 20(3):205-215.

[21] Jin H, Li Z J. Grid multi-scroll attractors in cellular neural network with a new activation function and pulse current stimulation[J]. *Nonlinear Dynamics*, 2025, 113(3): 2793-2810.

[22] Wu H G, Gu J X, Wang N, et al. Spiking and bursting activities in an NLAM-based CNN cell[J]. *Chaos, Solitons & Fractals*, 2025, 192: 115969.

[23] Zhang J, Liu E Z. Circuit design and image encryption of CNN chaotic system based on memristor[J]. *The European Physical Journal B*, 2024, 97(7): 100.

[24] Wang C H, Luo D W, Deng Q L, et al. Dynamics analysis and FPGA implementation of discrete memristive cellular neural network with heterogeneous activation functions[J]. *Chaos, Solitons & Fractals*, 2024, 187: 115471.

[25] Zhou X W, Jiang D H, de Dieu Nkapkop J, et al. Dynamics analysis and cryptographic implementation of a fractional-order memristive cellular neural network model [J]. *Chinese Physics B*, 2024, 33(4): 040506.

[26] Yu F, Su D, He S Q, et al. Resonant tunneling diode cellular neural network with memristor coupling and its application in police forensic digital image protection[J]. *Chinese Physics B*, 2025, 34(5): 050502.

[27] Zhang S, Zheng J H, Wang X P, et al. Initial offset boosting coexisting attractors in memristive multi-double-scroll Hopfield neural network [J]. *Nonlinear Dynamics*, 2020, 102(4): 2821-2841.

[28] Chen Y C, Tang C M, Yi Z X. A novel image encryption scheme based on PWLCM and standard map [J]. *Complexity*, 2020, 2020(1): 3026972.

[29] Wu H G, Zhang Y, Bao H, et al. Initial-offset boosted dynamics in memristor-sine-modulation-based system and its image encryption application [J]. *AEU-International Journal of Electronics and Communications*, 2022, 157: 154440.

[30] Liu X L, Tong X J, Wang Z, et al. A new *n*-dimensional conservative chaos based on generalized Hamiltonian system and its' applications in image encryption [J]. *Chaos, Solitons & Fractals*, 2022, 154: 111693.